A Quantum Chemical Study of the Catalysis for Cytidine Deaminase: Contribution of the Extra Water Molecule

Toshiaki Matsubara,*[,†,‡] Masashi Ishikura,[‡] and Misako Aida*[,†,‡]

Center for Quantum Life Sciences and Graduate School of Science, Hiroshima University, 1-3-1, Kagamiyama, Higashi-Hiroshima 739-8530, Japan

Received November 1, 2005

Cytidine deaminase is known as an important enzyme responsible for the hydrolytic deamination of cytidine, which is applied as a key step to the conversion of the precursor of the cancer drug to an active form in the living body. Cytidine with water is efficiently converted to uridine with ammonia in the cleft of cytidine deaminase. In this work, the catalysis of cytidine deaminase for the hydrolytic deamination was examined using cytosine as a model of cytidine and the model molecules for the active site of cytidine deaminase by means of the quantum chemical method. We especially investigated the contribution of the water molecule from the solvent to the catalysis, because the X-ray diffraction analysis of a crystal structure has revealed the existence of the water molecule in the vicinity of the substrate bound to the active site inside the cleft. Our computations showed that the extra water molecule from the solvent has a possibility to support the catalysis of cytidine deaminase.

1. INTRODUCTION

Cancer as well as AIDS (Acquired Immune Deficiency Syndrome), Alzheimer's disease, and so on is one of the most serious and intractable diseases and has distressed many people in the world for a long time. Many medical scientists have therefore always concentrated their efforts on the development of a sovereign remedy for this incurable disease with the up-to-date technology and science in the biological and the medical fields. However, unfortunately no specific medicine to completely cure the cancer has been found at this time. An immediate solution is strongly desired.

In recent years, capecitabine (pentyl [1-(3,4-dihydroxy-5-methyl-oxolan-2-yl)-5-fluoro-2-oxo-pyrimidin-4-yl]amino-formate), which is medicinal especially against metastatic breast cancer and colorectal cancer, has attracted much attention due to its excellent effectiveness. The oral therapy by tablet also popularized this medicine. Capecitabine is a cytotoxic antimetabolite that injures the cell through the RNA and DNA related mechanisms and interferes with the growth of the cancer cell. This is referred to as a 'masked compound', because it is a precursor of 5-fluorouracil (5-FU) active against the cancer cells. Capecitabine taken by mouth is converted to 5-FU within the living body. The conversion proceeds by some steps with the following enzymes: carboxyesterase, cytidine deaminase, and thimidine phosphorylase. Thimidine phosphorylase promoting the final step is mostly involved in the tumor tissues so that the active 5-FU is highly concentrated within the tumor tissues. Therefore, 5-FU selectively attacks the cancer cells to stop the growth and multiplication of the cells without destroying the normal and healthy tissues.

The conversion of 5′-deoxy-5-fluorocytidine (5′-DFCR) to 5′-deoxy-5-fluorouridine (5′-DFUR) by cytidine deaminase in the liver has been considered to be a key process on the design of the drug. So, a lot of studies concerning the function of cytidine deaminase have been accumulated.[1−21] The reaction formula of the hydrolytic deamination of cytidine is presented below.

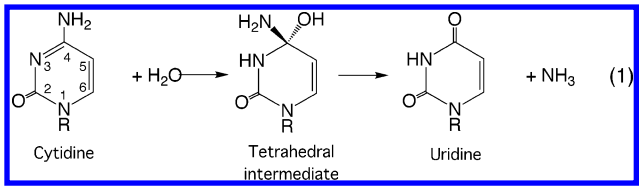

Uridine and ammonia is produced from cytidine and water. Cytidine deaminase efficiently promotes this reaction within the body. It is considered that the reaction starts with the addition of a water molecule to the N3═C4 double bond of cytidine and undergoes an intermediate usually referred to as the tetrahedral intermediate.[15−19] A water molecule would heterolytically dissociate and produce a proton and a hydroxyl anion. The proton and the hydroxyl anion add to the N3 and the C4 atoms, respectively, to form the tetrahedral intermediate in the first process. In the second process, uridine is produced with the release of ammonia. In the enzymatic reaction, cytidine is at first trapped and fitted in the cleft of cytidine deaminase. A reaction field produced in the cleft efficiently promotes the deamination.[15,17−19]

A lot of crystal structures registered in the data bank for citidine deaminase that bind a substrate analogue provide us with the information concerning its catalysis. On the basis of these data, we can speculate the mechanism of the deamination and the roles of amino acid residues in the active site. In the active site, an unsaturated Zn complex coordinated by a histidine and two cysteines is formed. The empty site of the Zn atom would bind with the incoming substrate and

* Corresponding author phone: +81 82 424 5735; fax: +81 82 424 5736; e-mail: matsu05@hiroshima-u.ac.jp.
† Center for Quantum Life Sciences.
‡ Graduate School of Science.

10.1021/ci050479k CCC: $33.50
Published on Web 03/02/2006

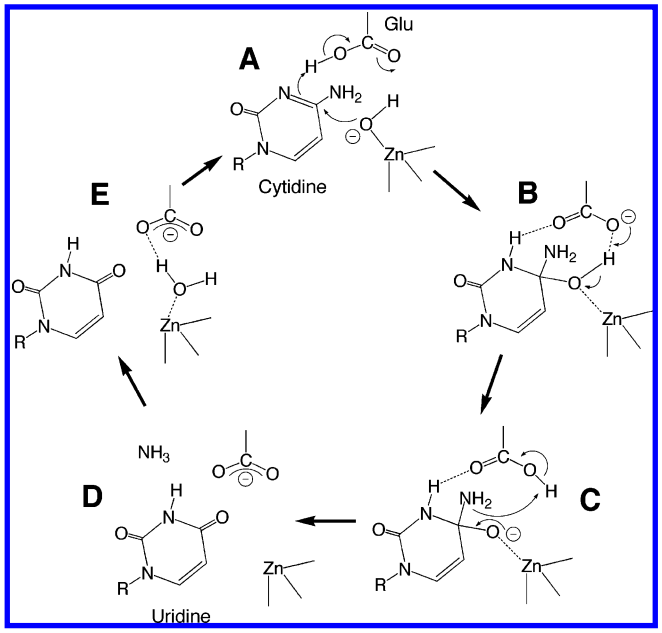

Figure 1. Proposed catalytic cycle of the hydrolytic deamination of cytidine in the active site of cytidine deaminase.

promote the deamination with the support of glutamic acid that is positioned in the vicinity of the substrate. A proposed full catalytic cycle of the hydrolytic deamination by cytidine deaminase[18,19] is presented in Figure 1. In the first step, **E** → **A**, a heterolytic dissociation of H_2O occurs. The incoming H_2O is at first bound to the empty site of the Zn complex. The O−H bond of the H_2O is cleaved, and the hydrogen is abstracted as a proton by the $-COO^-$ of glutamic acid. The formed hydroxyl anion on the Zn atom attacks the C4 atom of cytidine, and the −COOH hydrogen of glutamic acid is simultaneously transferred to the N3 atom of cytidine (**A** → **B**). As a result, the tetrahedral intermediate **B** is formed. The −OH hydrogen in **B** migrates to the $-NH_2$ group to form NH_3 and the product uridine (**B** → **C** → **D**). Glutamic acid is generally considered to play an important role on this hydrogen migration.

For the design and development of the wonder drug against the cancer, a complete understanding of the function of the enzyme is indispensable. We have therefore started for this purpose the theoretical examination of the catalysis of cytidine deaminase that is essential to activate capecitabine inside the human body. In the present study, we focused on the active site of cytidine deaminase and examined the mechanism of the hydrolytic deamination using a model system (cytosine + H_2O → uracil + NH_3) by means of the ab initio MO method. Molecular dynamics simulations of the enzymatic deamination in the real system are now in progress and will be separately reported elsewhere.

It is generally believed that the second process after the formation of the tetrahedral intermediate is rate-determining.[19,20] If this is true, then the proton migration in the tetrahedral intermediate from the −OH group to the $-NH_2$ group is a key step of the catalytic process. In this step, we examined the role of the extra water molecule from the solvent in addition to the role of the zinc atom and the glutamic acid from the enzyme, because we noticed that there is enough space to include some water molecules from the solvent in the cleft of the cytidine deaminase. As a matter of fact, the crystal structure registered in the Protein Data Bank (PDB code: 1AF2) indicates the existence of a water molecule in the vicinity of Glu104 inside the pocket of the active site.[21] It is therefore expected that the bound water inside the pocket of the active site not only fills the space up but also supports the catalysis as the contribution of the bound water to the transportation of the proton is known in the proton pumping in the biomolecular system.[22,23]

Following the explanation of the computational methods in section 2, we will discuss in section 3.1 the uncatalyzed hydrolytic deamination of cytosine. For the enzymatic deamination, we divide the catalytic cycle into two processes and discuss them separately. In section 3.2, at first, the second process of the catalytic cycle, i.e., the formation of uracile + NH_3 from the tetrahedral intermediate, which is considered to be a key process, is discussed. In section 3.3, the first process of the catalytic cycle, i.e., the formation of the tetrahedral intermediate starting from cytosine + H_2O, is discussed. Conclusions are summarized in the final section.

2. COMPUTATIONAL METHODS

All the calculations have been carried out using the GAUSSIAN03 program.[24] The geometry optimizations were performed at the B3LYP level of density functional theory, which consists of a hybrid Becke + Hartree−Fock exchange and a Lee−Yang−Parr correlation functional with nonlocal corrections,[25,26] adopting the 6-31G** basis set for all the atoms. All equilibrium and transitions state structures were fully optimized without any restriction and identified by the number of imaginary frequencies calculated from the analytical Hessian matrix. The higher quality basis set 6-311++G** was used to obtain more reliable energies for the second process of the catalytic cycle. The second-order Møller−Plesset perturbation (MP2) theory was also used for the geometry optimizations and the energy calculations for the equilibrium and the transition states optimized at the B3LYP/6-31G** level. The zero-point energies were calculated at the B3LYP level with a scale factor of 0.9614[27] for calculated vibrational frequencies. All the reaction coordinates were followed from the transition state to the reactant and the product by the intrinsic reaction coordinate (IRC) technique.[28] The natural bond orbital (NBO) analysis[29] was performed to obtain the charge distribution of the compounds. The active site of cytidine deaminase was simplified to CH_3COO^- + Zn, and cytosine was used as a model of cytidine. The complexes with CH_3COO^- have a negative charge of −1, and others are neutral.

3. RESULTS AND DISCUSSION

3.1. Uncatalyzed Hydrolytic Deamination of Cytosine. We assumed the hydrolytic deamination of cytosine without enzyme and examined its potential energy surface at the B3LYP/6-31G** level to compare with that of the enzymatic hydrolytic deamination. In the formation of uracil + NH_3 **7** starting from cytosine + H_2O **1**, two paths are possible as presented in Figure 2: path a passing through the tetrahedral intermediate **4a** (**1** → **4a** → **7**) and path b passing through the intermediate **4b** (**1** → **4b** → **7**). The experimentalists generally think path a for the enzymatic reaction. In path a, an incoming H_2O at first forms a complex **2a** with cytosine through the electrostatic interaction and adds to the N3═C4

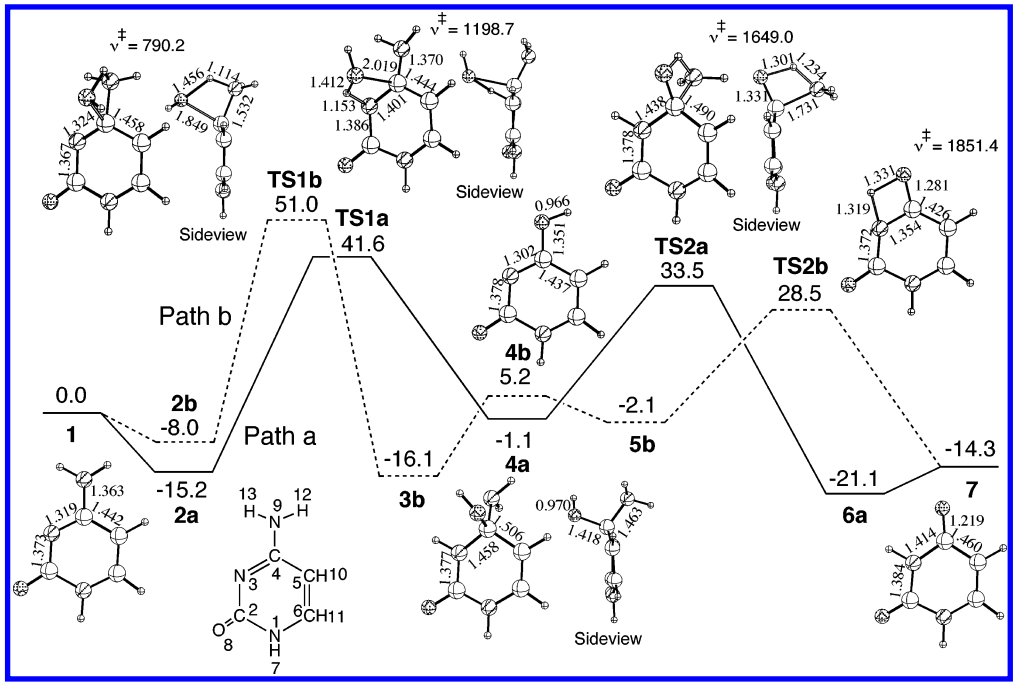

Figure 2. Potential energy surfaces (in kcal/mol) of the uncatalyzed hydrolytic deamination of cytosine together with the optimized structures (in Å) of the equilibrium and transition states at the B3LYP/6-31G** level. The solid line is for the reaction starting from the H_2O addition to the N3═C4 double bond of cytosine (path a: **1** → **4a** → **7**), and the dotted line is for the reaction starting from the H_2O addition to the C4−N9 bond of cytosine (path b: **1** → **4b** → **7**). **2a** and **2b** are the complexes of cytosine with H_2O formed by the electrostatic interaction between them. **3b** is the complex of the intermediate **4b** with NH_3 formed by the electrostatic interaction between them. **6a** is the complex of uracil with NH_3 formed by the electrostatic interaction between them. **5b** is the conformational isomer of **4b** where the hydrogen of the −OH group is on the opposite side to react through the transition state **TS2b**. The energies relative to cytosine + H_2O **1** are presented. The imaginary frequencies (in cm^{-1}) are presented for the transition states. The illustration of cytosine with the numbered atoms is displayed together for convenience.

double bond of cytosine to form the tetrahedral intermediate **4a**. The positively charged hydrogen and the negatively charged oxygen of H_2O are attracted by the negatively charged N3 and the positively charged C4 of cytosine, respectively. In the transition state **TS1a**, the water molecule is more strongly polarized by the contact with the highly negatively and positively charged N3(−0.602) and C4 (0.452). After a heterolytic dissociation of the O−H bond on the N3═C4 double, the hydroxyl anion adds to the C4 atom, and the proton migrates to the N3 atom with a lone pair electron. The C4 atom has a tetrahedral structure, and the distances of the C4−C5 and the N3−C4 bonds are stretched to 1.506 and 1.458 Å, respectively, in the intermediate **4a**, which shows that the orbital of the C4 atom is hybridized to sp^3. In the next step, uracil and NH_3 are produced from the tetrahedral intermediate **4a** with the migration of the −OH hydrogen to the $-NH_2$ nitrogen. The highly negatively charged N9 atom with a lone pair electron is the other candidate for the proton acceptor in the first step. In path b, therefore, the proton migrates to the N9 atom, and then a NH_3 molecule is released in the first step. In the subsequent step, uracil is produced from **4b** by the migration of the −OH hydrogen to the N3 atom through the intermediate **5b**. **5b** is the conformational isomer of **4b** where the hydrogen of the −OH group is on the opposite side to react through the transition state **TS2b**.

The potential energy surfaces of paths a and b in Figure 2 show the huge energy barriers for all steps of paths a and b. This is attributed to the structure of the transition state. All steps of paths a and b pass through the four-centered transition state as displayed in Figure 2. In such a cyclic transition state, the orbitals required for the bond dissociation and formation are deformed so much. This deformation largely increases the energy barrier. As we will see in the following sections, cytidine deaminase successfully reduces these large energy barriers in the active site. The intermediate **4a** of path a is more stable by 6.3 kcal/mol than the intermediate **4b** of path b. This stability of the intermediates, **4a** and **4b**, is reflected in the stability of the transition states, **TS1a** and **TS1b**, **TS1a** being more stable by 9.4 kcal/mol than **TS1b**. The difference in the stability between the intermediates **4a** and **4b** also affects the energetics of paths a and b. For path a, both first (**1** → **4a**) and second (**4a** → **7**) steps are exothermic. On the other hand, for path b, the first step (**1** → **4b**) is endothermic, although the second step (**4b** → **7**) is exothermic. In the enzymatic reaction, it is certainly expected in path a that the precedent proton migration to the N3 atom (see the Introduction and Figure 1) significantly enhances the electrophilicity of the C4 atom, and the subsequent nucleophilic attack of the hydroxyl anion becomes facile. We therefore selected path a in the subsequent sections to discuss the catalysis of cytidine deaminase.

Now, it is of great interest whether the energy barriers of paths a and b are reduced by the contribution of the extra water molecule, because the distortion in the structures of the transition states for the hydrogen transfer would be relaxed by the participation of the water molecule. As shown in Figure 3, the additional water molecule mediates the hydrogen transfer and forms a six-centered structure in each transition state. The six-centered transition state is thought to facilitate the orbital hybridization from the geometrical point of view. As expected, the energy barrier in each step

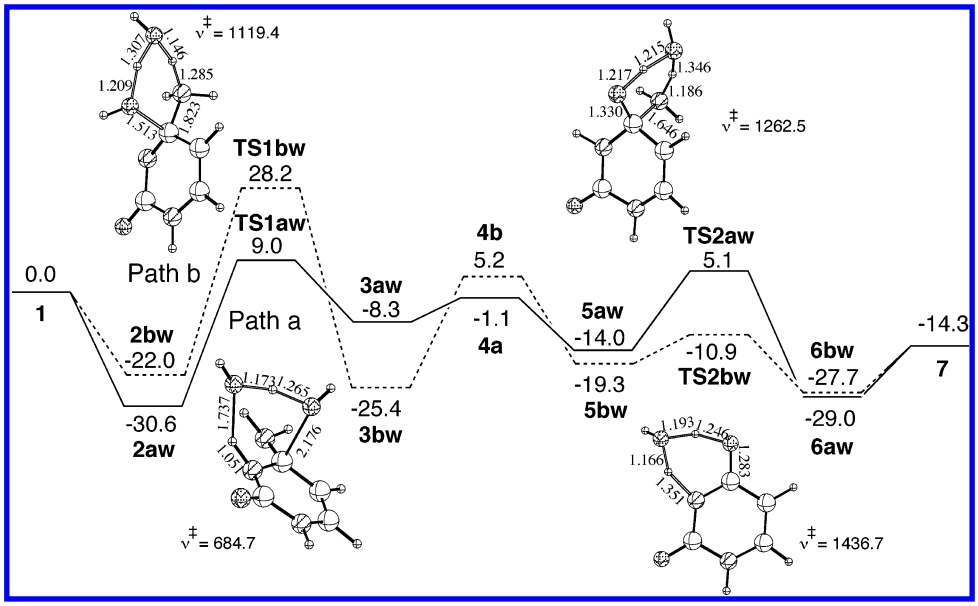

Figure 3. Potential energy surfaces (in kcal/mol) of the uncatalyzed hydrolytic deamination of cytosine with the additional water molecule together with the optimized structures (in Å) of the equilibrium and transition states at the B3LYP/6-31G** level. The solid line is for the reaction starting from the H_2O addition to the N3═C4 double bond of cytosine (path a: **1** → **4a** → **7**), and the dotted line is for the reaction starting from the H_2O addition to the C4−N9 bond of cytosine (path b: **1** → **4b** → **7**). **2bw** and **2aw** are the complexes of cytosine with $2H_2O$ formed by the electrostatic interaction among them. **3aw** and **5aw** are the complexes of the intermediate **4a** with H_2O formed by the electrostatic interaction between them. **3bw** and **5bw** are the complexes of the intermediate **4b** with $NH_3 + H_2O$ and the intermediate **5b** with H_2O, respectively, formed by the electrostatic interaction between them. **6aw** and **6bw** are the complexes of uracil with $NH_3 + H_2O$ and uracil with H_2O, respectively, formed by the electrostatic interaction between them. The energies relative to cytosine + $2H_2O$ **1** are presented. The imaginary frequencies (in cm^{-1}) are presented for the transition states. For the geometries of **1**, **4a**, **4b**, and **7** and the numbering of the atoms, see Figure 2.

more or less becomes smaller due to the stabilization of the transition state. This trend strongly appears in the second step of both paths a and b. However, all the energy barriers are still large. The entire potential energy surfaces of paths a and b except for the reactant **1** and the product **7** are stabilized by the interaction with the additional water molecule.

3.2. Formation of Uracil + NH_3 from the Tetrahedral Intermediate with Enzyme. In this and next sections, we discuss the hydrolytic deamination with enzyme. In this section, at first, we discuss the second process of the hydrolytic deamination, i.e., the formation of uracil from the tetrahedral intermediate, which is though to be a key process of the catalytic cycle.[19,20] As we have seen in the previous section (Figure 3), the second step of path a, **5aw** → **TS2aw** → **6aw**, has a large energy barrier of 19.1 kcal/mol. As a matter of course, it is our next issue whether this large energy barrier is really reduced by the contribution of the Zn atom and glutamic acid of cytidine deaminase. To make this point clear, we examined the potential energy surface of the hydrolytic deamination with the participation of the Zn atom and the glutamic acid.

According to the crystal structure (PDB code: 1AF2) observed by the X-ray diffraction,[21] we attach the Zn atom to the −OH oxygen and a glutamic acid to the H21 atom, as shown in Figure 4. Here, it is assumed that not a glutamic acid but a water molecule mediates the transfer of the −OH hydrogen to the $-NH_2$ nitrogen. When the Zn atom binds with the O15 atom in **8**, the energy barrier is reduced to 16.3 kcal/mol as shown by a (**8** → **TS3** → **9**) in Figure 4. The migration of the H16 to the N9 in a is slightly promoted by the effect of the Zn atom. However, the addition of CH_3COO^- to system a did not change the energy barrier so much as shown by b (**10** → **TS4** → **11**) in Figure 4. The hydrogen transfer is not promoted by the interaction of glutamic acid with cytosine. This suggests to us considering another contribution of glutamic acid, i.e., not the water molecule but the glutamic acid mediates the hydrogen transfer, as mentioned in the Introduction.

The optimized structures of the equilibrium and transition states of the formation of uracil from the tetrahedral intermediate where glutamic acid mediates the hydrogen transfer are presented in Figure 5. In the intermediate **12**, one of the oxygens (O17) of glutamic acid binds with the H21 atom. The other oxygen (O16) binds with the H20 atom. In the first step, **12** → **13**, the hydrogen H20 is abstracted by the O16 as a proton. It should be noted here that the $-NH_2$ group rotates around the C4−N9 axis in the course of this abstraction. The rotation of the $-NH_2$ group is a driving force of this step. Without this rotation, the hydrogen transfer in this step is uphill and does not proceed. The change in the potential energy surface of this step from **12** to **13** by the rotation of the $-NH_2$ group is presented in Figure S1 of the Supporting Information. The H20 attached to the O16 goes away from the O19 and comes close to the N9 to form a H-bond O16−H20- - -N9 with the help of glutamic acid in the next step, **13** → **14**. The H20 migrates to the N9 to form NH_3 in the final step, **14** → **15**. Throughout this reaction from **12** to **15**, the H-bond O17- - -H21−N3 is maintained, although its form is changed to O17−H21- - -N3 in **15**. The hydrogen H21 shifts its position and shuttles between two acceptors, the O17 and the N3, responding to the change in the H-bond network of the complex.

The potential energy surface is drastically changed compared to that of b in Figure 4 as presented in Figure 5. The energy barrier of each step is significantly reduced by the

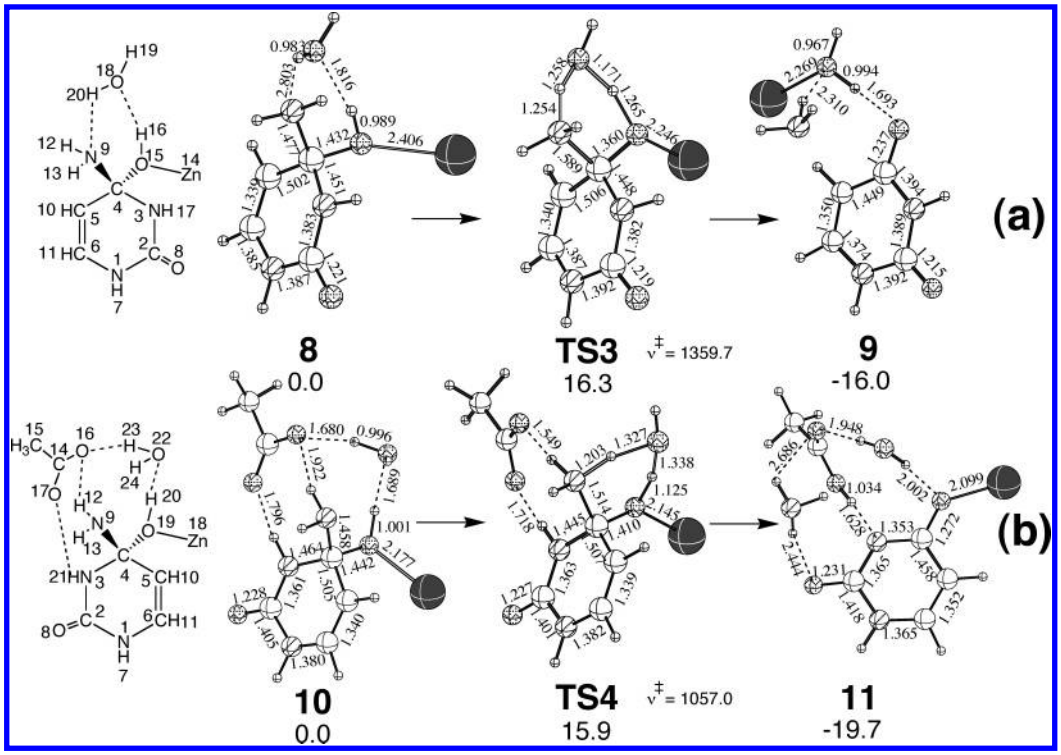

Figure 4. Optimized structures (in Å) of the equilibrium and transition states for the NH_3 formation from the tetrahedral intermediate and their relative energies (in kcal/mol) at the B3LYP/6-31G** level. The upper side (a) is for the reaction with the Zn atom and the lower side (b) is for the reaction with the Zn atom and the CH_3COO^- anion. The energies relative to **8** and **10** are presented for the reactions, a and b, respectively. The imaginary frequencies (in cm^{-1}) are presented for the transition states. The illustrations of the intermediates **8** and **10** with the numbered atoms are displayed together for convenience.

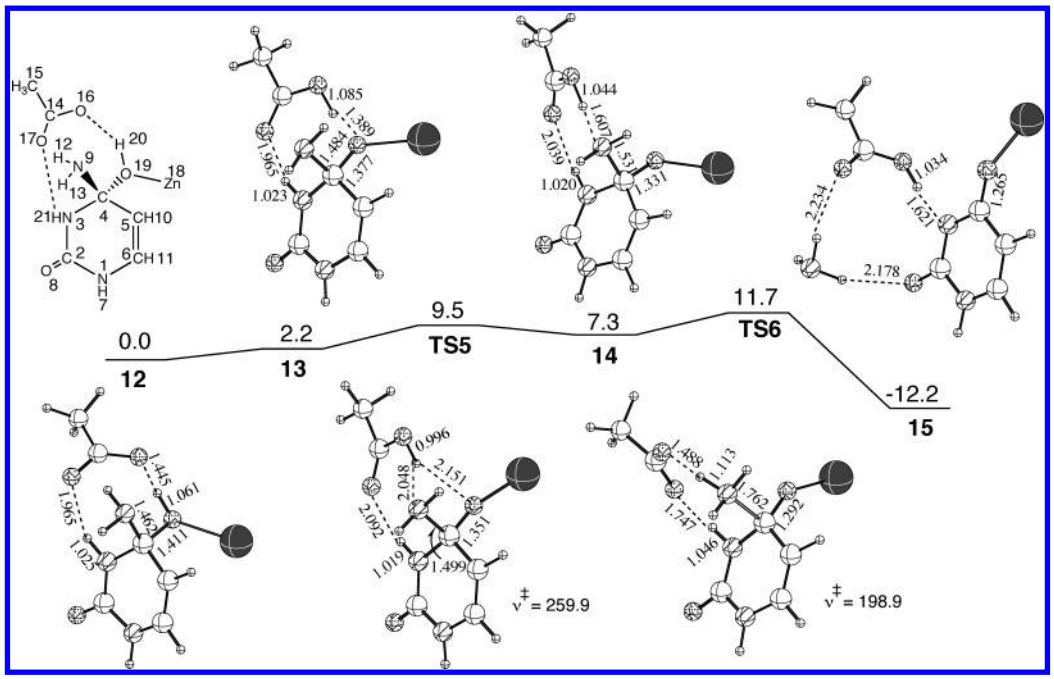

Figure 5. Potential energy surface (in kcal/mol) of the NH_3 formation from the tetrahedral intermediate with the Zn atom and the CH_3COO^- anion as a model of the active site of cytidine deaminase at the B3LYP/6-31G** level. The optimized structures (in Å) of the equilibrium and transition states at the B3LYP/6-31G** level are displayed together. The energies relative to the intermediate **12** are presented. The imaginary frequencies (in cm^{-1}) are presented for the transition states. The illustration of the intermediate **12** with the numbered atoms is displayed together for convenience.

mediation of glutamic acid so that the entire potential energy surface becomes smooth. The highest point at the transition state **TS6** of the NH_3 release is lowered by about 4 kcal/mol. The mechanism of the hydrogen transfer in Figure 5 is completely different from that of b in Figure 4. The transition state no longer has the four-centered structure. The hydrogen shuttles between two acceptors along the H-bond, passing through the transition state that has a linear structure. This is achieved with the support of glutamic acid.

As mentioned above, the X-ray diffraction analysis of the crystal structure revealed the existence of the water molecule from the solvent inside the pocket of the active site. This

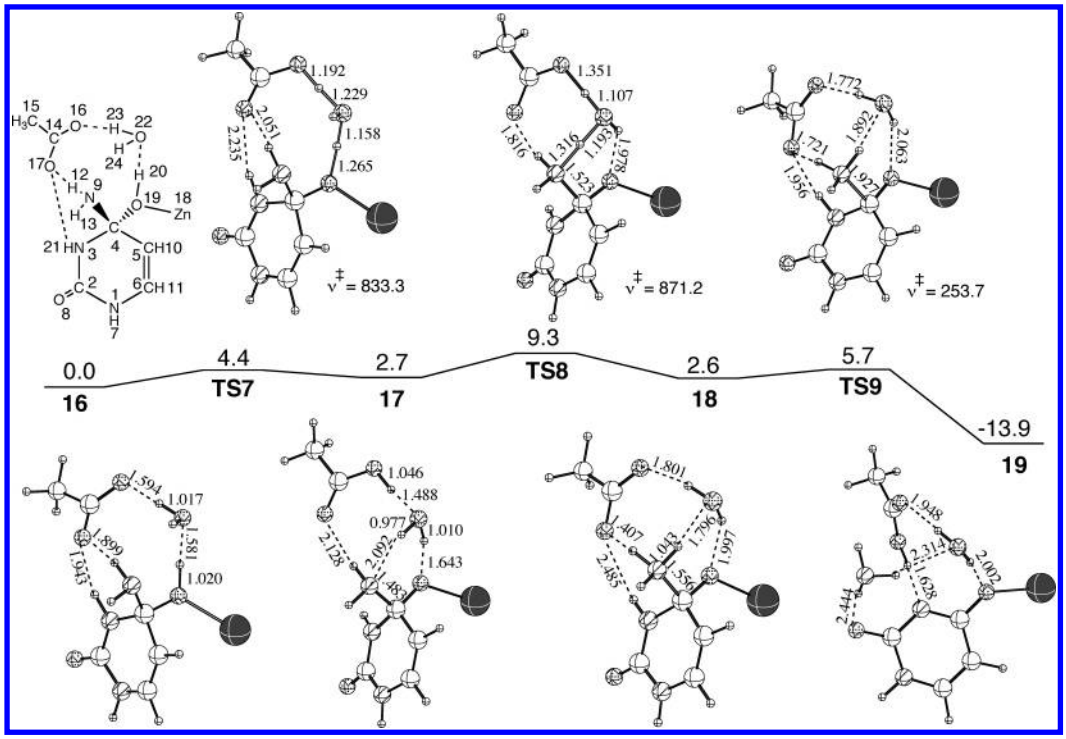

Figure 6. Potential energy surface (in kcal/mol) of the NH_3 formation from the tetrahedral intermediate with the Zn atom and the CH_3COO^- anion as a model of the active site of cytidine deaminase and the additional water molecule at the B3LYP/6-31G** level. The optimized structures (in Å) of the equilibrium and transition states at the B3LYP/6-31G** level are displayed together. The energies relative to the intermediate **16** are presented. The imaginary frequencies (in cm^{-1}) are presented for the transition states. The illustration of the intermediate **16** with the numbered atoms is displayed together for convenience.

suggests that some water molecules come inside the pocket to fill the space up as a bound water. Does this bound water participate to the reaction? This is now our question. To obtain an answer to this question, we assumed a mechanism, in which the extra water molecules from the solvent in addition to the glutamic acid from the enzyme participate to the mediate the hydrogen transfer, and examined the effect of the extra water molecules on the deamination (Figure 6).

In the starting intermediate **16**, the water molecule occupies the space produced between the O16 and the H20 atoms and forms the H-bonds, O16- - -H23−O22 and O22- - -H20−O19. The H20 and the H23 atoms synchronously shift to the O22 and the O16, respectively, to form the intermediate **17**. The H24−N9 distance shortens to 2.092 Å, while the H20−O19 distance lengthens to 1.643 Å in **17**, because the water molecule slides a little into the side of the N9 atom. Consequently, the water molecule bridges the O19 and the N9 atoms. In the step, **17** → **18**, the hydrogen migrates from the O16 to the N9. Since the movement of the H23 and the H24 is asynchronous, a hydronium ion H_3O^+ is formed in the transition state **TS8**. The produced NH_3 molecule is bound to the C4 atom in the intermediate **18** due to the high electrophilicity of the C4 atom and forms a coordinate bond with the C4 atom sharing its lone pair electron. At the MP2 level, one of the NH_3 hydrogens was transferred to the O17 in **18** (see Figure S2 of the Supporting Information). In the last step, **18** → **19**, NH_3 dissociates with the hybridization of the orbital on the C4 atom. *One can notice that the proton migration takes place along the H-bond like a proton pumping that has been found in the biomolecular system.*[22,23] *The present system transports the proton utilizing the H-bond network. The extra water molecule supports this transportation changing the structure of the H-bond network to make a path of the proton migration.*

The entire potential energy surface becomes more smooth compared to that without the contribution of the extra water molecule. The transition state in each step is stabilized. It is obvious that the deamination is enhanced by the participation of the extra water molecule. The feature of the entire potential energy surface was not changed by the geometry optimizations of the equilibrium and the transition states at the MP2 level (see Figure 2S of the Supporting Information). The single-point energy calculations at the MP2/6-31G** level for the optimized geometries at the B3LYP/6-31G** level also showed a similar potential energy surface as presented in Table 1. The inclusion of the zero-point energy slightly shifts up the energy surface for the hydrogen migration step from **16** to **18**. On the other hand, the basis set 6-311++G** including a diffuse function for all the atoms shifts the energy surface down. The transition state **TS7** disappeared due to its stabilization with this basis set.

We also examined a possible mediation of two extra water molecules in the hydrogen transfer. The calculated path is presented in Figure 7. In the tetrahedral intermediate **20**, one extra water molecule occupies the space produced between the O16 and the H20 atoms and forms two H-bonds, O16- - -H23−O22 and O22- - -H20−O19, which is similar to the case of the system with one extra water molecule (see **16** in Figure 6**)**. The other extra water molecule bridges the H24 and the N9 atoms forming two H-bonds, O25- - -H24−O22 and N9- - -H26−O25. The reaction starts from the proton migration from the O19 to the O16 (**20** → **21)**. The proton is not transported by one step along the H-bond network, O19−H20- - -O22−H24- - -O25−H26- - -N9. At first, the H20 and the H23 atoms shift to the O22 and the O16 atoms,

Table 1. Relative Energies of the Equilibrium and Transition States of the NH_3 Formation Starting from **16** and **20** at the B3LYP and MP2 Levels[a]

	E[b]		E + Corr.1[c]		E + Corr.2[d]		E + Corr.1 + Corr.2	
complex	B3LYP	MP2	B3LYP	MP2	B3LYP	MP2	B3LYP	MP2
16	0.0	0.0	0.0	0.0	0.0	0.0	0.0	0.0
TS7	4.4	5.1	7.1	7.7	0.7	1.4	3.4	4.1
17	2.7	2.0	5.1	5.4	2.2	2.4	4.7	4.9
TS8	9.3	11.5	12.0	14.2	6.0	8.2	8.8	11.0
18	2.6	3.1	3.6	4.0	1.9	2.3	2.9	3.3
TS9	5.7	9.3	5.3	8.9	4.9	8.5	4.5	8.1
19	−13.9	−10.4	−16.1	−12.5	−16.3	−12.7	−18.4	−14.9
20	0.0	0.0	0.0	0.0	0.0	0.0	0.0	0.0
TS10	2.8	3.9	5.9	6.9	0.1	1.2	3.1	4.2
21	−1.2	−0.2	2.3	3.3	−1.5	−0.5	2.0	3.0
TS11	0.0	1.4	4.8	6.2	−1.9	−0.5	2.9	4.2
22	−4.3	−5.2	−3.5	−4.4	−3.4	−4.4	−2.7	−3.6
TS12	2.6	4.6	8.4	10.4	0.5	2.5	6.3	8.3
23	−0.8	0.0	2.7	3.5	−0.7	0.1	2.7	3.5
TS13	3.0	4.4	7.7	9.1	1.1	2.5	5.8	7.2
24	−1.0	−0.9	0.8	0.9	−0.4	−0.3	1.5	1.5
TS14	3.9	8.0	2.4	6.5	3.6	7.7	2.1	6.2

[a] All the energies were calculated for the optimized geometries at the B3LYP/6-31G** level. [b] Potentioal energies with the basis set 6-31G**. [c] Corr.1 = zero-point energy at the B3LYP/6-31G** level for each equilibrium and transition state. [d] Corr.2 = the energy difference, *E*(at B3LYP/6-311++G**) − *E*(at B3LYP/6-31G**), for each equilibrium and transition state.

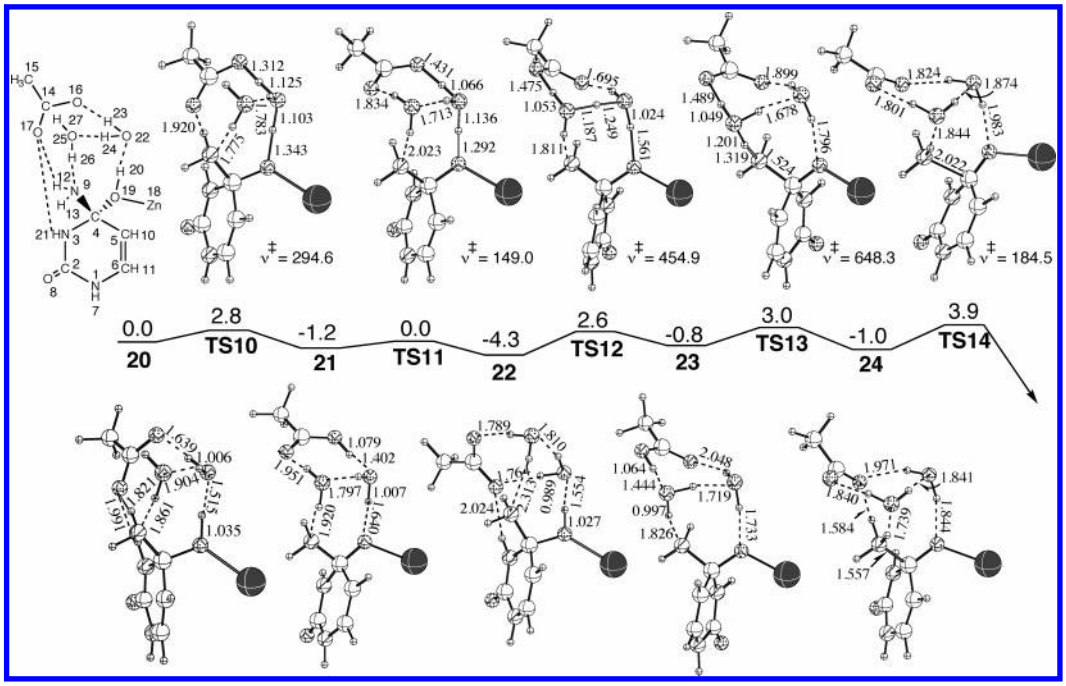

Figure 7. Potential energy surface (in kcal/mol) of the NH_3 formation from the tetrahedral intermediate with the Zn atom and the CH_3COO^- anion as a model of the active site of cytidine deaminase and two additional water molecules at the B3LYP/6-31G** level. The optimized structures (in Å) of the equilibrium and transition states at the B3LYP/6-31G** level are displayed together. The energies relative to the intermediate **20** are presented. The imaginary frequencies (in cm^{-1}) are presented for the transition states. The illustration of the intermediate **20** with the numbered atoms is displayed together for convenience.

respectively, on the H-bond network O19−H20- - -O22−H23- - -O26. Since the movement of two hydrogen atoms are stepwise, the hydronium ion H_3O^+ is formed in the transition state TS10. During this step, the O17- - -H21−N3 H-bond is broken, and the new H-bond O17- - -H27−O25 is formed by the move of the O17 to the H27. This rearrangement of the H-bond arises from the change in the electronic structure of the $-COO^-$ by receiving the proton.

One would intuitionally assume two possible paths in the proton migration from the O16 to the N9; one utilizing two H-bond networks, O16−H23- - -O22−H24- - -O25−H27- - -O17 and O17−H27- - -O25−H26- - -N9, one after the other, and the other utilizing one H-bond network O16−H23- - -O22−H24- - -O25−H28- - -N9. However, in fact, both paths are impossible, because the H-bond network in **21** is partially broken and rearranged with the dissociation of the proton from the O16. The proton returns to the O19 atom in the next step, **21** → **22**, passing through the transition state **TS11** of which the structure is similar to that of **TS10** except for the position of the O17 atom. The O17 atom slightly changes its position and comes more close to the H27 atom. In contrast, the O16 atom drastically changes its position and

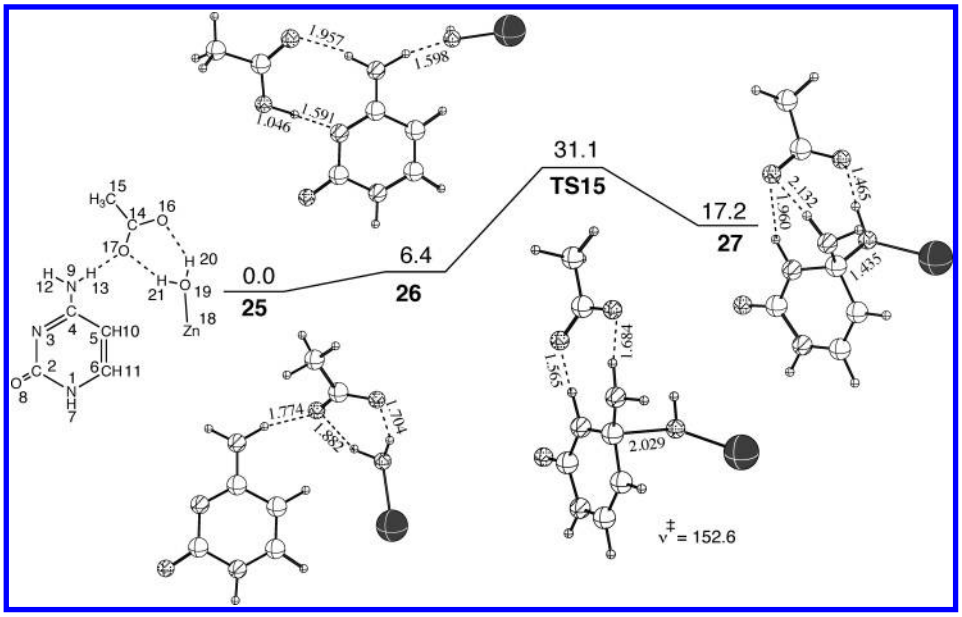

Figure 8. Potential energy surface (in kcal/mol) of the tetrahedral intermediate formation from cytosine + H_2O with the Zn atom and the CH_3COO^- anion as a model of the active site of cytidine deaminase at the B3LYP/6-31G** level. The optimized structures (in Å) of the equilibrium and transition states at the B3LYP/6-31G** level are displayed together. The energies relative to **25** are presented. The imaginary frequencies (in cm^{-1}) are presented for the transition states. The illustration of **25** with the numbered atoms is displayed together for convenience.

comes close to the H21 atom. As a result, the H-bond network is rearranged, and a new H-bond, O16- - -H21−N3, is formed in the intermediate **22**. In this way, the H-bond is switched, and its network is arranged at every moment to make a path of the proton migration. In **22**, the proton migrates from the O19 to the O17 utilizing the H-bond network, O19−H20- - -O22−H24- - -O25−H27- - -O17, to form **23**. The H-bond N3−H21- - -O16 is broken during this reaction. The proton is passed from the O17 to the N9 in the subsequent step, **23** → **24**, and NH_3 is released in the last step. The O16 atom comes close to the H12 atom to form a H-bond in **24**. The complex to be formed after the dissociation of NH_3 was not found, because it is converted to an unrealistic structure. Thus, the proton transportation is achieved by shifting the hydrogen one by one on the H-bond network formed by the participation of the extra water molecules. This finding by computations is similar to the proton pumping that has been found in the living system.[22,23]

Compared to the case of the reaction with one extra water molecule, the transition state of every step is more stable in energy, and the entire potential energy surface is quite smooth, as shown in Figure 7. The highest point at the transition state **TS14** in the NH_3 release is only 3.9 kcal/mol higher than the starting intermediate **20**. The potential energy surface calculated at the MP2 level also shows a similar feature as presented in Table 1. By the zero-point correction, the energy surface except for the last step is shifted up. The energy surface calculated with the higher quality basis set 6-311++G** becomes more smooth, because the transition states except for **TS14** are more stabilized by 2−3 kcal/mol. The calculated energy surfaces that have the highest point at the transition state of the NH_3 release or in its precedent step are in agreement with the experimental results and then verify that the present model is adequate.

3.3. Formation of the Tetrahedral Intermediate Starting from Cytosine + H_2O with Enzyme. The first process of the catalytic cycle to form the tetrahedral intermediate is discussed in this section. The optimized structures of the equilibrium and transition states and the potential energy surface of this process without the additional water molecule are presented in Figure 8. As mentioned in the Introduction, the first step of this process is the dissociation of the water molecule. The Zn atom, which forms a three-coordinate complex with a histidine and two cysteines in the real system, binds with a water molecule in its active site to enhance the dissociation. One of the hydrogens is abstracted as a proton by the $-COO^-$ of glutamic acid and the OH^- remains on the Zn atom. The dissociated proton is transported by glutamic acid to the N3 atom, in the step, **25** → **26**. We did not follow this step completely in this study using the ab initio MO method. But, the quantum mechanical MD study for the simulation of the reaction including this step is now in progress. The nucleophile Zn−OH oxygen attacks the positively charged C4 atom in the next step. The energy of 31.1 kcal/mol required to reach to the transition state **TS15** is very large. Most of the energy is spent to break the O19- - -H13−N9 H-bond of **26**. In fact, the energy needed for the formation of the C4−O19 bond after the breaking of the O19- - -H13−N9 H-bond was calculated to be only 1.4 kcal/mol. In the real system, it is assumed that the reaction field inside the cleft of the enzyme makes the nucleophilic attack of Zn−OH oxygen facile controlling the position of the Zn atom from enzyme, because it is generally believed in experiment that the second process after the formation of the tetrahedral intermediate is rate-determining.

By the participation of two additional water molecules, the move of glutamic acid would be minimized. The hydrogen of the H_2O coordinated to the Zn atom moves to the N3 through the H-bond network as presented in Figure 9. The migration of the H21 to the N3 consists of two steps. In the first step, **28** → **29**, the proton (H21) from H_2O is transferred to the O17 by the shift of the hydrogen on the H-bond network O19−H21- - -O22−H24- - -O25−H26- - -

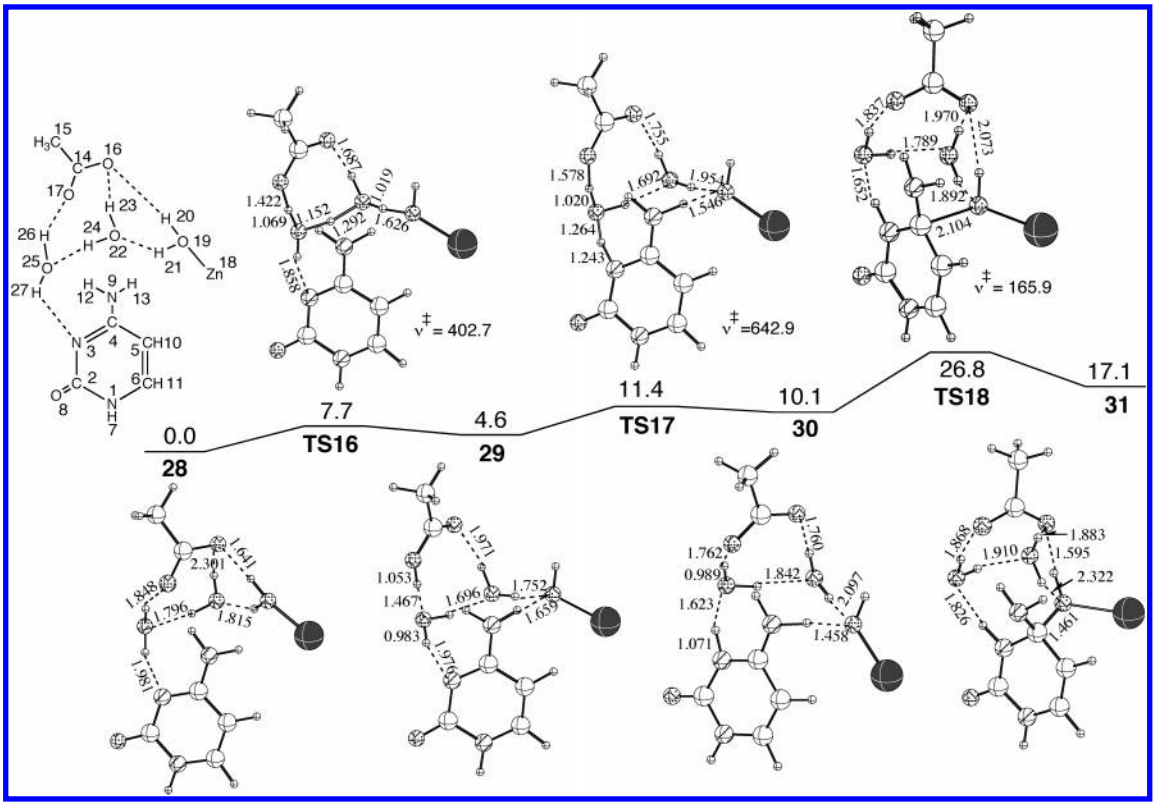

Figure 9. Potential energy surface (in kcal/mol) of the tetrahedral intermediate formation from cytosine + H_2O with the Zn atom and the CH_3COO^- anion as a model of the active site of cytidine deaminase and two additional water molecules at the B3LYP/6-31G** level. The optimized structures (in Å) of the equilibrium and transition states at the B3LYP/6-31G** level are displayed together. The energies relative to **28** are presented. The imaginary frequencies (in cm^{-1}) are presented for the transition states. The illustration of **28** with the numbered atoms is displayed together for convenience.

O17. In the second step, **29** → **30**, the proton finally shifts to the N3 along another H-bond network O17−H26- - -O25−H27- - -N3. Path of the migration from the O19 to the N3 by one step does not exist. The nucleophilic attack of the Zn−OH oxygen to the C4 atom occurs in the last step, **30** → **31**. The entire potential energy surface becomes smooth compared to the case of the reaction without the participation of the extra water molecules. However, the top of the mountain at the transition state **TS18** is still 26.8 kcal/mol higher in energy than the intermediate **28**. We suppose that this feature of the energy surface is changed, and the height of the mountain is reduced in the pocket of the active site of the real enzyme, because the sterically relaxed H-bonding network before reaching to **TS18** would be affected and destabilized by the steric effect of the amino acid residues in the real system.

4. CONCLUDING REMARKS

In this study, we proposed a new mechanism of the enzymatic hydrolytic deamination with the participation of the extra water molecules from the solvent by the quantum chemical method. Our calculations suggested that the catalysis of cytidine deaminase is effectively enhanced by the participation of the extra water molecule. The key process of the hydrolytic deamination is the migration of the proton dissociated from the water molecule. The glutamic acid from the enzyme mediates the proton migration. Consequently, the energy barrier of the proton migration is reduced, and the hydrolytic deamination is promoted. When the extra water molecules participate to this process, the proton is transported in the different way. A H-bond network is formed in the complex of the substrate, glutamic acid, and water molecules from the solvent. The proton is transported by the shift of the hydrogen on the H-bond network. This is similar to a proton pumping which has been found in the biomolecular system within the human body. The transition states are further stabilized, and the energy surface becomes quite smooth with the participation of the extra water molecules. As far as we know, this is a first report suggesting the contribution of the extra water molecules from the solvent to the catalysis of cytidine deaminase on the hydrolytic deamination. Our new findings in this work are quite useful for the drug design for the deamination.

ACKNOWLEDGMENT

The calculations were in part carried out at the Computer Center of the Institute for Molecular Science of Japan. This study was partly supported by grants from the Ministry of Education, Culture, Sports, Science and Technology of Japan.

Supporting Information Available: The change in the potential energy and the geometry of the intermediate **12** by the rotation of the $-NH_2$ group around the C4−N9 axis (Figure S1), the optimized structures of the equilibrium and transition states and the potential energy surface of the step, **16** → **19**, at the MP2/6-31G** level (Figure S2), and listings giving the optimized Cartesian coordinates of all equilibrium structures and transition states in this paper. This material is available free of charge via the Internet at http://pubs.acs.org.

REFERENCES AND NOTES

(1) Evans, B. E.; Mitchell, G. N.; Wolfenden, R. Action of bacterial cytidine deaminase on 5,6-dihydrocytidine. *Biochemistry* **1975**, *14*, 621−624.

(2) Wentworth, D. F.; Wolfenden, R. Interaction of 3,4,5,6-tetrahydrouridine with human liver cytidine deaminase. *Biochemistry* **1975**, *14*, 5099−5105.

(3) Liu, P. S.; Marquez, V. E.; Driscoll, J. S.; Fuller, R. W.; McCormack, J. J. Cyclic urea nucleosides. Cytidine deaminase activity as a function of aglycon ring size. *J. Med. Chem.* **1981**, *24*, 662−666.

(4) Vita, A.; Amici, A.; Cacciamani, T.; Lanciotti, M.; Magni, G. Cytidine deaminase from *Escherichia coli* B. Purification and enzymic and molecular properties. *Biochemistry* **1985**, *24*, 6020−6024.

(5) Frick, L.; Yang, C.; Marquez, V. E.; Wolfenden R. V. Binding of pyrimidin-2-one ribonucleoside by cytidine deaminase as the transition-state analog 3,4-dihydrouridine and contribution of the 4-hydroxyl group to its binding affinity. *Biochemistry* **1989**, *28*, 9423−9430.

(6) Smith, A. A.; Carlow, D. C.; Wolfenden, R.; Short, S. A. Mutations affecting Transition-State Stabilization by Residues Coordinating Zinc at the Active Site of Cytidine Deaminase. *Biochemistry* **1994**, *33*, 6468−6474.

(7) Xiang, S.; Short, S. A.; Wolfenden, R.; Carter, C. W., Jr. Transition-state selectivity for a single hydroxyl group during catalysis by cytidine deaminase. *Biochemistry* **1995**, *34*, 4516−4523.

(8) Xiang, S.; Short, S. A.; Wolfenden, R.; Carter, C. W., Jr. Cytidine Deaminase Complexed to 3-Deazacytidine: A "Valence Buffer" in Zinc Enzyme Catalysis. *Biochemistry* **1996**, *35*, 1335−1341.

(9) Carlow, D. C.; Short, S. A.; Wolfenden, R. Complementary Truncations of a Hydrogen Bond to Ribose Involved in Transition-State Stabilization by Cytidine Deaminase. *Biochemistry* **1998**, *37*, 1199−1203.

(10) Carlow, D. C.; Carter, C. W., Jr.; Mejlhede, N.; Neuhard, J.; Wolfenden, R. Cytidine Deaminases from *B. subtilis* and *E. coli*: Compensating Effects of Changing Zinc Coordination and Quaternary Structure. *Biochemistry* **1999**, *38*, 12258−12265.

(11) Snider, M. J.; Lazarevic, D.; Wolfenden, R. Catalysis by Entropic Effects: The Action of Cytidine Deaminase on 5,6-Dihydrocytidine. *Biochemistry* **2002**, *41*, 3925−3930.

(12) Johansson, E.; Neuhard, J.; Willemoes, M.; Larsen, S. Structural, Kinetic, and Mutational Studies of the Zinc Ion Environment in Tetrameric Cytidine Deaminase. *Biochemistry* **2004**, *43*, 6020−6029.

(13) Pham, P.; Bransteitter, R.; Goodman, M. F. Reward versus Risk: DNA Cytidine Deaminases Triggering Immunity and Disease. *Biochemistry* **2005**, *44*, 2703−2715.

(14) Chung, S. J.; Fromme, J. C.; Verdine, G. L. Structure of Human Cytidine Deaminase Bound to a Potent Inhibitor. *J. Med. Chem.* **2005**, *48*, 658−660.

(15) Snider, M. J.; Gaunitz, S.; Ridgway, C.; Short, S. A.; Wolfenden, R. Temperature Effects on the Catalytic Efficiency, Rate Enhancement, and Transition State Affinity of Cytidine Deaminase, and the Thermodynamic Consequences for Catalysis of Removing a Substrate "Anchor". *Biochemistry* **2000**, *39*, 9746−9753.

(16) Carlow, D. C.; Short, S. A.; Wolfenden, R. Role of Glutamate-104 in Generating a Transition State Analogue Inhibitor at the Active Site of Cytidine Deaminase. *Biochemistry* **1996**, *35*, 948−954.

(17) Carlow D. C.; Smith, A. A.; Yang, C. C.; Short, S. A.; Wolfenden R. Profound contribution of a carboxymethyl group to transition-state stabilization by cytidine deaminase: Mutation and rescue. *Biochemistry* **1995**, *34*, 4220−4224.

(18) Betts, L.; Xiang, S.; Short, S. A.; Wolfenden, R.; Carter, C. W., Jr. Cytidine Deaminase. The 2•3 Å Crystal Structure of an Enzyme: Transition-state Analog Complex. *J. Mol. Biol.* **1994**, *235*, 635−656.

(19) Snider, M. J.; Reinhardt, L.; Wolfenden, R.; Cleland, W. W. ^{15}N Kinetic Isotope Effects on Uncatalyzed and Enzymatic Deamination of Cytidine. *Biochemistry* **2002**, *41*, 415−421.

(20) Yao, L.; Li, Y.; Wu, Y.; Liu, A.; Yan, H. Product Release Is Rate-Limiting in the Activation of the Prodrug 5-Fluorocytosine by Yeast Cytosine Deaminase. *Biochemistry* **2005**, *44*, 5940−5947.

(21) Xiang, S.; Short, S. A.; Wolfenden, R.; Carter, C. W., Jr. The Structure of the Cytidine Deaminase-Product Complex Provides Evidence for Efficient Proton Transfer and Ground-State Destabilization. *Biochemistry* **1997**, *36*, 4768−4774.

(22) Alberts, B.; Johnson, A.; Lewis, J.; Raff, M.; Roberts, K.; Walter, P. *Molecular Biology of the Cell*, 4th ed.; Garland Science: New York, 2002.

(23) Nelson, D. L.; Cox, M. M. *Lehninger Principles of Biochemistry*, 3rd ed.; Worth: New York, 2000.

(24) Frisch, M. J.; Trucks, G. W.; Schlegel, H. B.; Scuseria, G. E.; Robb, M. A.; Cheeseman, J. R.; Montgomery, J. A., Jr.; Vreven, T.; Kudin, K. N.; Burant, J. C.; Millam, J. M.; Iyengar, S. S.; Tomasi, J.; Barone, V.; Mennucci, B.; Cossi, M.; Scalmani, G.; Rega, N.; Petersson, G. A.; Nakatsuji, H.; Hada, M.; Ehara, M.; Toyota, K.; Fukuda, R.; Hasegawa, J.; Ishida, M.; Nakajima, T.; Honda, Y.; Kitao, O.; Nakai, H.; Klene, M.; Li, X.; Knox, J. E.; Hratchian, H. P.; Cross, J. B.; Adamo, C.; Jaramillo, J.; Gomperts, R.; Stratmann, R. E.; Yazyev, O.; Austin, A. J.; Cammi, R.; Pomelli, C.; Ochterski, J. W.; Ayala, P. Y.; Morokuma, K.; Voth, G. A.; Salvador, P.; Dannenberg, J. J.; Zakrzewski, V. G.; Dapprich, S.; Daniels, A. D.; Strain, M. C.; Farkas, O.; Malick, D. K.; Rabuck, A. D.; Raghavachari, K.; Foresman, J. B.; Ortiz, J. V.; Cui, Q.; Baboul, A. G.; Clifford, S.; Cioslowski, J.; Stefanov, B. B.; Liu, G.; Liashenko, A.; Piskorz, P.; Komaromi, I.; Martin, R. L.; Fox, D. J.; Keith, T.; Al-Laham, M. A.; Peng, C. Y.; Nanayakkara, A.; Challacombe, M.; Gill, P. M. W.; Johnson, B.; Chen, W.; Wong, M. W.; Gonzalez, C.; Pople, J. A. *Gaussian 03*; Gaussian, Inc.: Pittsburgh, PA, 2003.

(25) Lee, C.; Yang, W.; Parr, R. G. Development of the Colle-Salvetti correlation-energy formula into a functional of the electron density. *Phys. Rev. B* **1988**, *37*, 785−789.

(26) Becke, D. Density-functional thermochemistry. III. The role of exact exchange. *J. Chem. Phys.* **1993**, *98*, 5648−5652.

(27) Scott, A. P.; Radom, L. Harmonic Vibrational Frequencies: An Evaluation of Hartree−Fock, Mller−Plesset, Quadratic Configuration Interaction, Density Functional Theory, and Semiempirical Scale Factors. *J. Phys. Chem.* **1996**, *100*, 16502−16513.

(28) Fukui, K.; Kato, S.; Fujimoto, H. Constituent analysis of the potential gradient along a reaction coordinate. Method and an application to methane + tritium reaction. *J. Am. Chem. Soc.* **1975**, *97*, 1−7.

(29) Glendening, E. D.; Reed, A. E.; Carpenter, J. E.; Weinhold F. *NBO Version 3.1*.

CI050479K